FERMILAB-CONF-05-607-CD

Radial Tail Resolution in the SELEX RICH

A. Morelos[a] *, J.Mata[a], P.S. Cooper[b], J.Engelfried[a], J.L. Aguilera-Servin[a]

[a]Universidad Autónoma de San Luis Potosí, México

[b]Fermi National Accelerator Laboratory, Batavia Illinois 60510

We use a 7 Million event data sample of 600 GeV/c single track pion events, where the pion track is reconstructed upstream and downstream of the SELEX RICH. We build the RICH ring radius histogram distribution and count the tail events that fall outside 5σ, giving a fraction of 4×10^{-5} events outside the Gaussian tails. This control of events establishes the ability of using the RICH as velocity spectrometer for high precision searches of the $K^+ \to \pi^+ \nu \bar{\nu}$ decay like it is planned in the CKM experiment.

PACS: 29.40.Ka

Keywords: RICH detector

1. Introduction

Two RICH velocity spectrometers have been proposed by the CKM collaboration [1–3]. The CKM goal is a 5 % measurement on the V_{td} element of the CKM matrix. CKM requires the detection of 100 $K^+ \to \pi^+ \nu \bar{\nu}$ decay events to reach its goal.

On top of the signal there is a much more copious $K^+ \to \pi^+ \pi^0$ decay. To separate the signal region a level of 3×10^{-5} in the fraction of RICH ring radius tail events is required.

SELEX RICH single track data have been used to quantify the radius distribution tails. The present work is an improved version of a previously reported result in the CKM proposal [1], where a level of 7.9×10^{-5} fractionial events was reached using only the existence of the track upstream of the RICH detector.

2. SELEX

Figure 1 shows the relevant SELEX detectors used in this study. Each event was triggered by beam scintillators located upstream of the scattering targets. The particle is tracked by a magnetic spectrometer located upstream of the RICH. The magnet is surrounded by wire chambers and silicon strip detectors. In order to remove unwanted decays we selected events where only one track is fit all the way from the beam region to the wire chambers. To remove multiple track events we selected events with a single segment found in the wire chambers. In order to guaranty the track existence downstream of the RICH we used a set of position detectors named Vector Drift Chambers (VDC A and B). We extrapolated the upstream track to determine the existence of hits in the VDC chambers and then fit a straight line to them. We joint the upstream and downstream segments to form a single track when the opening angle is less than 0.2 mrad.

We make use of the SELEX Total Cross Section Measurement data [4]. The data consist of 600 GeV/c single particle events. The data are approximately half π^- and half Σ^-, with a contamination of K^- and Ξ^- at the 1 % level. We make use of the Beam Transition Radiation Detector, BTRD, to select only pions as the $\beta = 1$ particle crossing the entire $\approx$ 60 m length of the SELEX spectrometer.

*Talk presented at the 5th. International Workshop on Ring Imaging Cherenkov Counters (RICH2004), November 2004, Playa del Carmen, Q.R., Mexico

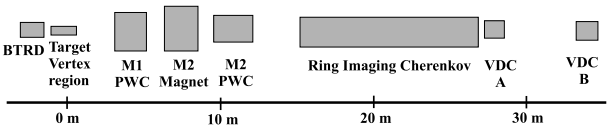

Figure 1. SELEX spectrometer schematic.

3. SELEX RICH

The RICH configuration, parameters, and properties have been previously reported [5,6]. The general features are described in the following lines.

The RICH detector consists of a 10.22 m long vessel filled with Ne gas. Cherenkov light was reflected on a 2.4 m × 1.2 m spherical mirror of 19.8 m radius and 10 mm thickness. The mirror was built from 16 hexagonal pieces, each one 40 cm across. The photon detector located at the focal plane consists of 2848 1/2 in phototubes. The phototubes were arranged in a matrix of 89 columns by 32 rows. Two different brands of phototubes were used, Hamamatsu R760 and FEU60. The central part of the matrix had alternated columns of each brand of tubes, the outer part had only FEU60 tubes.

SELEX uses upstream track information to locate the ring center on the photon detector. A likelihood algorithm assigns the ring radius and locate phototubes on the ring for different charged lepton, meson and hyperon hypothesis.

The measured single hit resolution is 5.5 mm. The contributions come from: matrix pixel size, 4.04 mm; upstream PWC resolution, 3.0 mm; mirror alignment, 2.06 mm; and dispersion in neon, 1.2 mm. The ring radius resolution measured for the case of single tracks is 1.5 mm, while for the multitrack case it is 1.8 mm.

In the SELEX RICH all particle species at 600 GeV/c are considered to have the same radius within the above measured resolution. At this momentum the Ω^- differs by 3.4 mm from the $\beta = 1$ ring radius, while the electron, μ and π ring radius overlap at 11.5 cm.

4. Radius Distributions and Tails

Candidate phototubes are selected from a circular band of ±1.27 cm centered on the circle found by the SELEX likelihood method. Using the ring center and radius as free parameters a fit with error handling is performed on the candidate phototubes [7,8]. This algorithm reduces the single hit resolution to 0.47 cm by removing the upstream PWC contribution.

We build the radius distribution and apply a multi-Gaussian fit to it. Three common parameters are used to describe each Gaussian: number of entries under the curve (p_1); average radius (p_2); and single hit resolution (p_3). The fitting multi-Gaussian function is:

$$g = p_1 \sum_i f_i \frac{1}{\sqrt{2\pi s_i^2}}\ e^{-\frac{1}{2}(\frac{x-p_2}{s_i})^2}\ ; s_i = \frac{p_3}{\sqrt{i-3}}$$

where i is the number of phototubes on the ring; f_i weights each Gaussian by the number of events corresponding to each i.

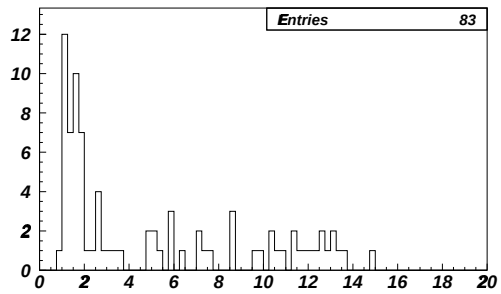

Figure 2. Reduced χ^2 distribution obtained from fitting one multi-Gaussian set to each run data sample. Half the runs show a systematic feature.

We verified the quality of our data by splitting the data in subsamples by run number. We applied the multi-Gaussian fit to each radius distribution subsample. From the reduced χ^2 distribution (Fig. 2) we found that half the runs fit well

a multi-Gaussian set and the other half has a systematic feature, yet uncovered. We also measured the dispersion on the radius average; it amounts to 0.009 cm; well below the single track resolution. We defined this dispersion as the σ obtained by fitting a Gaussian to a histogram whose entries are the mean radius of each subsample.

The radius distribution for the full data sample is shown in Fig. 3 and Fig. 4. Figure 3 corresponds to the case where only the existence of the upstream track has been established. Figure 4 shows the case where the existence of track goes all the way downstream of the RICH. We choose to fit two multi-Gaussian sets over the full data sample radius distribution in order to get an acceptable χ^2. Each one of the two multi-Gaussian sets has its own center, width and height as explained above.

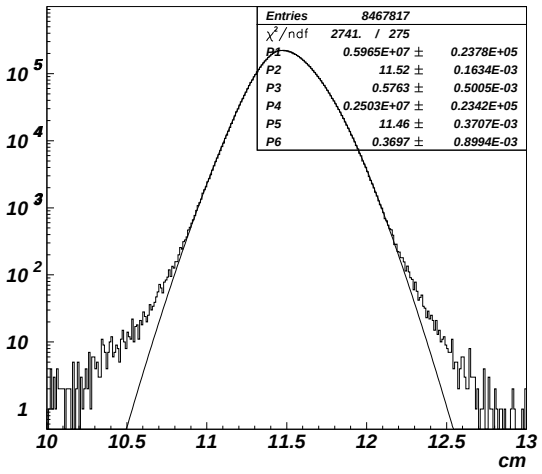

Figure 3. Ring radius Distribution, upstream track.

The relevance of Fig. 4 is the reduction on the tail event population compared to Fig. 3. We define as tail region in the radius distribution all but the central radius region between 10.6 and

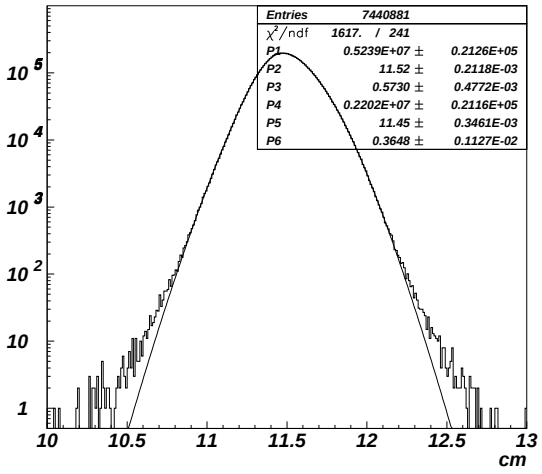

Figure 4. Ring radius Distribution, upstream and downstream track.

12.4 cm. The central region corresponds to 10 times the worst case multitrack radius resolution. In the tail region we count 677 events or a fraction of 7.99×10^{-5} for Fig. 3. The tail region of Fig. 4 has 297 events or a fraction of 3.99×10^{-5}. We remove half tail events while losing 12.13% data due to VDC reconstruction efficiency. This fraction of events is very close to the CKM experiment requirements.

We model the expected decay events we may discard requiring the downstream track existence. We take into account possible Σ^- and K^- decays that may happen inside the RICH. The decays are restricted to pass our candidate phototube selection criteria and they are outside our joint upstream - downstream segment definition. These decays fall in a window of 0.2 to 0.85 mrad in the decay opening angle. The π^- decay is not considered due to the fact that the opening angle between the π^- and μ^- is well below 0.2 mrad.

Table 1 summarizes the results of the model. We obtain 600 events which are discarded as decays by the upstream - downstream concatenation. This should be compared against the mea-

sured difference in the tails of figures 3 and 4 which accounts for 300 decay events, taking into account the VDC inefficiency loss.

We use an extended radius distribution tail region, defined by all but the central radius region between 11.0 and 12.0 cm. We now define as tail events the absolute difference between the data and the fitting curve. We found 3561 tail events outside the fitting curve for Fig. 3 and 2195 tail events for Fig. 4. The difference between those tail events amount for 934 decay events after correcting for VDC inefficiency.

The fact that we are removing hundreds of events with the VDC track existence is in agreement with a decay model inside the RICH. Our new algorithm selects better single track $\beta = 1$ events.

baryon/meson (>8 BTRD planes)	0.0015
Σ^- at downstream end of RICH	3044.36
Σ^- at upstream end of RICH	4903.17
Σ^- decaying inside of RICH	1857.81
Σ^- decays not discarded by RICH	379.36
Σ^- decays discarded by VDC	354.7
K^- decays discarded by VDC	304
Total events discarded by VDC	~ 660

Table 1
Interpretation model of discarded decay events.

The kind of events left on the tail radius distribution region have predominantly a "C" like shape, with all the phototubes in half of the ring, as shown in Fig. 5. Contrary to "C" like events, the events that are near de average radius have plenty of phototubes distributed on the ring. The "C" like events either reduce or enlarge the circle depending on its own distribution and noise around the ring.

5. Photon Detector Simulation

A simulation of the phototube distribution on the RICH photon detector was made with the following considerations: a ring radius of 11.51 cm;

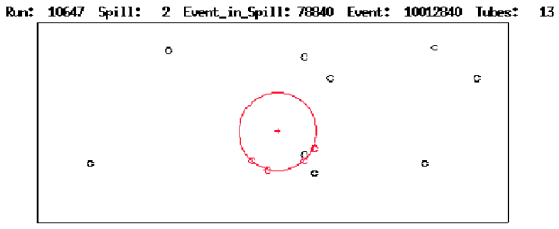

Figure 5. Typical event in radius distribution tail, "C" like form. Ring and PMT's found by SELEX likelihood method.

the number of phototubes given by a Poisson distribution with a mean of 11.96; the phototube angular position on the ring randomly flat distributed; the x and y phototube position dispersed by a Gaussian distribution of $\sigma = 0.44$ cm; and excluding overlapped simulated phototubes.

We added noise on the ring by switching on one of the six neighboring tubes with a 0.25 probability. In addition, we added random noise to the whole phototube array with a probability of 0.0023, equivalent to 13.5 kHz. At this stage we did not take into account the difference on configuration, efficiency and noise between phototube brands. Table 2 compares the ring radius, number of phototubes on the ring, and total number of phototubes for simulation and data. There is fairly good agreement between phototube detector data and simulation.

distribution	simulation mean, RMS	data mean, RMS
radius [cm]	11.53, 0.19	11.49, 0.15
PMT's on ring	11.75, 3.01	11.65, 3.01
PMT's total	19.32, 4.13	19.27, 4.18
No. events	261198	316017

Table 2
Photon detector simulation and data.

We show the maximum angular separation of

hits in a ring in Fig. 6 for simulation and data. The distributions peak around around $\frac{1}{2}\pi$ radians. The fraction of events with a maximum angular separation of $> \pi$ radians is 0.00145 and 0.00137, respectively. The maximum angular separation let us appreciate how randomly nature produces the "C" type events.

6. Summary

SELEX RICH single track data have been used to quantify the ring radius distribution tail. The present work is an improved version over the already one reported in the CKM proposal, where the fraction of tail events was 7.9×10^{-5}. By requiring the existence of the track downstream of the RICH we reduced the sample by 12.13 % and we pushed down the fraction of tail events to 3.99×10^{-5}. This level of precision is close to the requirements of high precision experiments like CKM.

The number of rejected tail events are in agreement with Σ^- and K^- decays in the RICH. These decays are in a window of 0.2 to 0.85 mrad in the angle between the two charged particles of each decay.

The kind of events left on the tail radius distribution region have all the phototubes in half of the ring. The phototube array resemble a "C" shape. The effect of the "C" type events will be reduced, in future experiments, by using efficient and the less noisy brand tubes to avoid deformation on the ring fit. The "C" type events that remain with a better detector are a-priori identifiable and can be cut with a rather small loss if necessary.

Acknowledgments

The authors thank the SELEX collaboration, the SELEX RICH group and the technical staff of their Institutions for the great performance of the RICH and the quality of the accumulated SELEX data. This work was supported by the US Department of Energy under contract no. DE-AC02-76CHO3000, the Russian Ministry of Science and Technology, and Consejo Nacional de Ciencia y Tecnologia (Mexico).

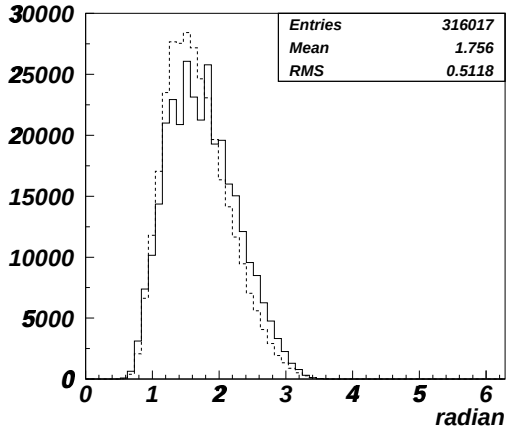

Figure 6. Maximum angle between two consecutive PMT's. Continuous line, Entries, Mean and RMS are data. Dotted line is simulation.

REFERENCES

1. J. Frank et al., Charged Kaons at the Main Injector, A Proposal for a Precision Measurement of the Decay $K^+ \to \pi^+ \nu \bar{\nu}$ and Other Rare K^+ Processes at Fermilab Using the Main Injector, 2nd Edition, Fermi National Accelerator Laboratory, Batavia, IL, USA, April, 2001. www.fnal.gov/projects/ckm/Welcome.html
2. J. Engelfried, et al., Nucl. Instr. and Meth. A 502, 62, 2003.
3. P. Cooper, Redesign of the CKM RICH Velocity Spectrometers for use in an unseparated 1/4 GHz beam, this RICH2004 Conference.
4. U. Dersch, et al., Nucl. Phys. B 579, 277, 2000.
5. J. Engelfried, et al., Nucl. Instr. and Meth. A 431, 53, 1999.
6. J. Engelfried, et al., Nucl. Instr. and Meth. A 502, 285, 2003.
7. J.F. Crawford, Nucl. Instr. Meth. 211, 223, 1983.
8. P. Cooper, Fitting RICH Rings, CKM_33, CKM Internal Note, 2000.